Journal of Scientific & Industrial Research
Vol. 82, September 2023, pp. 925-931
DOI:10.56042/jsir.v82i9.3991

# Influence of Textile Layer Positioning on Flexural Strength- An Insight towards Field Casting of Textile Reinforced Concrete

Shankar* & Gopinath

CSIR-Structural Engineering Research Centre, Chennai 600 113, India

*Received 06 December 2021; revised 28 June 2023; accepted 15 July 2023*

As advancements in the construction industry demand fresh applications of thin-walled structures, Textile Reinforced Concrete (TRC) holds significant potential in the field and is yet to be explored thoroughly. The present experimental research investigates the effect of the position of the textile layer across the cross-section of TRC, which is a significant aspect while field casting of TRC products. The investigation is carried out for two different volume fractions initially, with two layers of textile placed in three distinct textile layer positions by performing 4-Point Bending (4PB) tests. The three types are, providing two layers at the bottom tension zone (2B), providing two layers at the center of the cross-section (2M), and providing one layer at the top compression zone and one at the bottom tension zone (1T1B). The study also attempts to arrive at a standardized analytical method to calculate the flexural capacity of cross-sections with different textile layer positions. From the experiment and analytical results, it was evident that the 2B type arrangement yielded approximately around 20% more capacity than 2M and around 50% more than 1T1B arrangements.

This study also explores the pattern in the flexural capacity of the TRC section with the above three-layer positions, varying different volume fractions. The relationship between the volume fraction and flexural capacity and the influence of both volume fraction and textile position in cross-section on the flexural capacity is also explored. It is observed that the percentage difference in flexural capacity between 1T1B and 2B is relatively uniform for all volume fractions considered whereas the difference between 2M and 2B decreases till a volume fraction of 0.85% after which the difference staggers around an average value of 28.8%. The study establishes an advantageous layer positioning system across the cross-section, thereby increasing the capacity of the cross-section. Consequently, besides optimizing the utilization of the cross-section, this approach can directly lead to the most economical thickness for all applications involving the flexural strength of TRC.

**Keywords:** Analytical method, Flexural capacity, Layer arrangement, Textile layer, Volume fraction

## Introduction

Conventional steel-reinforced concrete is a prevalent construction material due to many of its advantages. One of the few significant disadvantages of steel-reinforced concrete is the necessity of adequate concrete cover for the reinforcement to prevent its corrosion. The durability of the material is predominantly dependent on preventing the reinforcement from corrosion employing sufficient cover which increases the size and thereby the weight of the element and the structure as a whole. Textile Reinforced Concrete (TRC) is an alternative building material that effectively resolves the issue as the reinforcements used are non-metallic and the demand for concrete cover is very less. Thus, by reducing the thickness of the members considerably, TRC effectively reduces the self-weight and increases the durability of the structure. Thinner sections also facilitate ease of material to be molded into different shapes as per the requirement, enabling various applications such as shell structures[1] and piping.[2] The possibility to produce thin, lightweight, durable elements makes TRC a competitive material to be used in pre-cast structures and can be employed in applications such as large-sized façade panels[3,4] and modular constructions.[5] TRC is also used to retrofit structures,[6,7] strengthen masonry structures[8,9] and sandwich panels.[10,11]

Various research papers are published on the characterization of TRC and one of the most important behavior is the response of TRC under flexural load. Most of the applications require the material to exhibit reasonable flexural strength and the ability to calculate the capacity realistically would aid to design an efficient, thinner section that would be easier to handle and transport. Being a non-homogenous material, TRC has a complex distribution of stress across the section and length

*Author for Correspondence
E-mail: shankarnaren23@gmail.com

which necessitates in-depth study on its response and behavior to realize the design of structural elements with TRC.

For the well - established steel-reinforced concrete, the position of the steel reinforcement governs the flexural capacity of the section. The position of the reinforcement across the cross-section alters the lever arm of the flexural moment and consequently the capacity. Present study focuses to capture a similar behavior in TRC where a considerable advantage in flexural strength can be achieved by varying the position of the textile layer across the cross-section. In addition to providing the most advantageous section, this would also enable us to include a factor of safety in design with the same cross-section through adequate quality control. The paper also attempts to arrive at a standard analytical approach based on the work of Alrshoudi[12], to calculate the flexural capacity of the section, sensitive to the position of textile layers. The analytical method yields fairly similar values to the experimental results. The analytical formula automatically incorporates a factor of safety required for a conservative design. Then employing the same analytical expression, pattern of variation of flexural capacity for various volume fractions is explored with respect to the above three textile positions.

## Experimental Investigation

To understand the effect of position of layers across the cross-section, 4-point bending (4PB) tests are done on samples where the position of the layers is varied. Two layers of textiles are kept at three different positions across the cross-section and its impact is observed and studied. Three positions contemplated are, two layers of textile placed near bottom surface of cross-section (tension zone) (2B), two layers placed at the center of the cross-section (2M) and one layer placed near bottom surface and one placed near top surface of the cross-section (1T1B). Specimens are cast with two volume fractions ($v_f$), 0.85% and 1%, to perceive the effect of volume fraction on flexural capacity with different textile layer positions. The textiles are of 12.5 mm mesh and are coated with locally obtained chemicals with proven binding capacity to glass fibers. The matrix of the specimens is made as per *Gopinath et al.*[13] The specimens are cast with dimensions 450 × 100× 15 mm ($SP_{15}$) and 450 × 100 × 18mm ($SP_{18}$). For specimen type 2B, 2 textile layers are kept at 5mm and 6mm from bottom for $SP_{15}$ and $SP_{18}$ specimen respectively. For specimen 1T1B, one textile layer is kept each at the distance of 5mm and 6mm from top and bottom surface for $SP_{15}$ and $SP_{18}$ specimen respectively. The specimens are prepared in steel moulds using hand lay-up technique. The specimen is removed from mould after one day and cured under water for 28 days. At least two specimens are cast for each type. Image of a typical specimen is as shown in Fig. 1 and 4-point bending test set up is as shown in Fig. 2. A Universal Testing Machine (UTM) Material Testing System, of capacity 7.5T is used to apply the load gradually on the specimen. The rate of loading could be adjusted and it was set as +1 mm/min. UTM plots the relationship between the load applied and the corresponding displacement of the specimen continuously. Roller supports are provided at both ends to establish a simply supported beam. Two rollers are placed at the top of the specimen at a distance of 100mm from the support to apply the point load. Thick steel plates are placed above the rollers to ensure equal load transfer.

The specimen is 450 mm long to facilitate the test setup with support's center to center length being 300 mm. Point load is applied at 100 mm (300/3) from both the supports setting up a region of pure flexure between the point loads. The load is gradually applied until failure. The typical 4PB set-up followed is as

Fig. 1 — Typical specimen for 4PB

Fig. 2 — Test set up for 4PB

shown in Fig. 3. After the specimen fails the flexural capacity ($M_e$) of the section is calculated from the maximum load with the following Eq. (1).

$$M_e = \frac{WL}{6} \quad \dots (1)$$

where, W is the maximum load, L is the distance between the supports of the specimen.

The nomenclature adopted for the specimens are as given in Table 1.

## Results and Discussion

The load is applied gradually at the rate of +1 mm/min until failure. The failure is primarily characterized by one major crack and few minor cracks. The major crack is predominantly observed near one of the loading positions. The cracks formedand the subsequent failure is depicted in Fig. 4 (a–c). The crack initiates from the bottom (tension zone) and gradually propagates towards the top (compression zone). Complete failure is observed when the crack reaches the top. The damage of the textile layers can also be distinctly spotted after the failure. Apart from the major cracks propagating from the tension side to the compressive side, eventually to the top surface of the section, few minor cracks initiated from the tension side but are not observed to reach the top surface of the compression zone. All the cracks formed are as expected in the pure flexure zone, i.e., between the two loads. Minor cracks developed enable dissipation of energy which evidently increases the capacity of the section. The damage of the textile demonstrates that the specimen has reached the second and third stage of a typical TRC stress-strain response where the load is carried by both matrix and textile and only textile respectively.

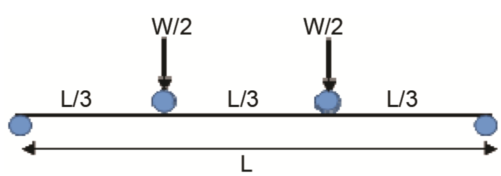


Fig. 3 —Typical 4PB test setup

A similar conclusion can also be drawn from Fig. 5 (a & b) which illustrates the flexural response with the load-displacement curve. The undulations in the graph indicate the cracks formed at those stages. It confirms that multiple cracks are formed during these stages before failing.It can be observed that 2B type specimen not only exhibits higher ultimate load but also significantly higher displacement before reaching the ultimate load than 2M and 1T1B specimen. It's also observed that an increase in the thickness of the specimen yields a significant difference in the ultimate load of specimen for both 2B and 2M whereas, in the case of 1T1B, the increase of both ultimate load and total displacement is minimal. The displacement post ultimate load is especially high for

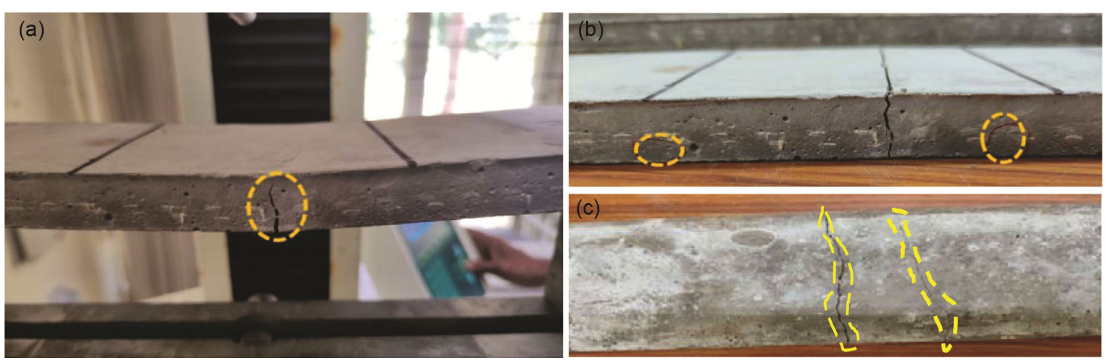


Fig. 4 — (a) Crack propagating from bottom, (b) Minor cracks formed, Cracks formed at bottom surface

Table 1 — Specimen Nomenclature

| Textile position | Depth of the cross-section | Nomenclature | Remark |
|---|---|---|---|
| Two layers of textiles near bottom (2B) | 15 mm | 2B15 | Both textile layers at 5 mm from bottom surface |
| | 18 mm | 2B18 | Both textile layers at 6 mm from bottom surface |
| Two layers of textiles at centre (2M) | 15 mm | 2M15 | Both textile layers at centre |
| | 18 mm | 2M18 | Both textile layers at centre |
| One layer near top and one near bottom (1T1B) | 15 mm | 1T1B15 | One textile layer kept at 5 mm from top and bottom surface |
| | 18 mm | 1T1B18 | One textile layer kept at 6 mm from top and bottom surface |

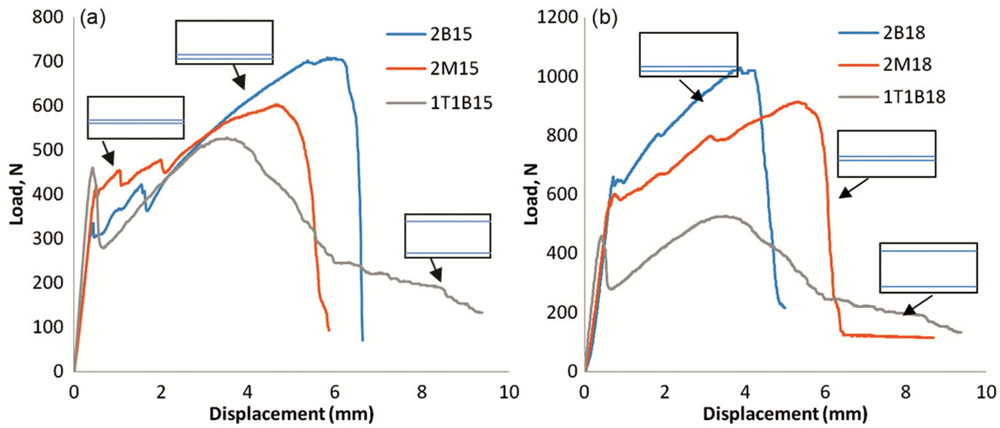


Fig. 5 — Load displacement curve: (a) –$SP_{15}$, (b) –$SP_{18}$

1T1B case for both 15mm and 18mm thick specimens. It is also important that the ultimate load carried by 1T1B is lesser than the counterparts for both thicknesses. Since the preferable response on any typical application would require material to accommodate sufficient displacement before reaching the ultimate load, it can be positively established that among 2B, 2M, and 1T1B, the former two types are always preferable to the latter. It can also be observed in Fig. 5 (a&b) that for both 2B and 2M cases, there is a very steep fall after the ultimate load, whereas 1T1B the fall is gradual. This might be attributed to the textile layer available at the top. For 2B and 2M cases, since both the textiles are present at same position, both fail simultaneously and hence a steep fall after the ultimate load, whereas for 1T1B, the textile layer at top is virtually undamaged till the failure of the textile at bottom tension zone. After the failure of textile at tension zone, it can be speculated that some flexure is carried by the remaining textile layer and that is the reason the fall is not steep for 1T1B as in the case of the other two configurations.

**Comparison with Analytical Method**

An analytical method to calculate the bending moment capacity of TRC section is attempted with the view to generalize it and arrive at the most advantageous position of textile layer across the cross- section. The analytical calculation is based on the method proposed by Alrshoudi.[12]The study evaluates the flexural capacity of the section based on a similar methodology as of steel reinforced concrete. The technique requires the section to be under reinforced as expected in the conventional steel reinforced concrete. The provided reinforcement ratio, ρ (Area of textile/Area of cross-section) has to be less than the balanced reinforcement ratio, $\rho_{fb.}$ The balanced reinforcement ratio is given by Eq. (2),

$$\rho_{fb} = 0.85\beta_1 \frac{f_c'}{f_{fu}} (\frac{\varepsilon_{cu}}{\varepsilon_{cu}+\varepsilon_{fu}}) \quad \ldots (2)$$

where, $\varepsilon_{cu}$ is ultimate strain of Concrete, $\varepsilon_{fu}$ is ultimate strain in fibre, $f_{fu}$ is the ultimate tensile strength of textile fibre, $f_c$' is the mean compressive strength of the concrete, and $\beta_1$ is given by the Eqs 3(a&b),

$$\beta_1 = 0.85 \text{ when } f_c' \leq 27.5 \text{ MPa} \quad \ldots (3a)$$

$$\beta_1 = 0.85 - 0.05\left(\frac{f_c'-27.5}{7}\right) \text{ when } f_c' \geq 27.5 \text{ MPa} \quad \ldots (3b)$$

However, $\beta_1$ is always ≥ 0.65.

Thus, after making sure, $\rho_{fb} \geq \rho$, the flexural capacity of the section is given by Eq. (4),

$$M_{n=}\eta_\tau \rho b d^2 f_{fu}(1 - 0.59\frac{\eta_\tau \rho f_{fu}}{f_c'}) \quad \ldots (4)$$

where, $\eta_\tau$ is the efficiency factor, b is the width of the section and d is the effective depth of the section. In the following study, efficiency is considered as 0.4.

Using above Eqs (2,3 & 4) the flexural capacity of section $SP_{15}$ and$SP_{18}$ are calculated. The comparison between moment capacities obtained from analytical calculations using Eq. (4) and values from experiments using Eq. (1) are compared in Fig. 6 (a & b).

From the Fig. 6 (a & b), we can recognize that the pattern is similar in both experimental and analytical capacities for both $SP_{15}$ and $SP_{18}$ sections. For both thicknesses, the maximum flexural capacity is achieved in the 2B section and the least capacity is the result of the 1T1B configuration. The main criterion for opting to experiment 1T1B case is to check the contribution of the textile in the compression zone. The experimental results along with the analytical results convincingly demonstrate that placing textiles in the compression zone do not actively participate in increasing the flexural capacity. The pattern

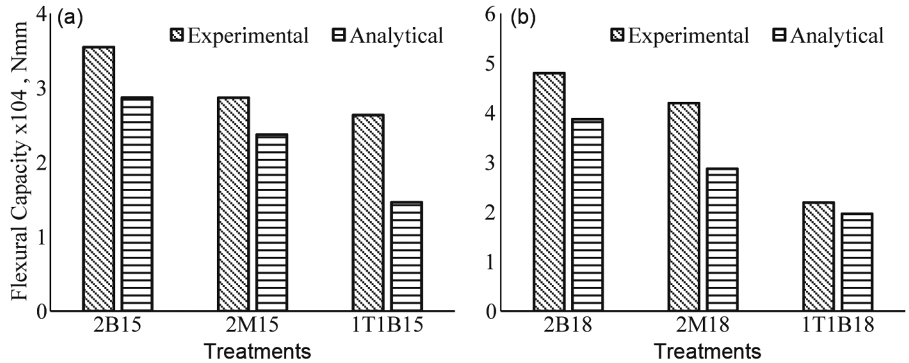


Fig. 6 — Flexural capacity comparison: (a) –$SP_{15}$, (b) –$SP_{18}$

recognized from Fig. 6 (a & b) also validates the analytical calculations. Although the values are lesser, the behaviour is similar where maximum flexural capacity is achieved from the 2B type and the least from the 1T1B type. This also logically substantiates that the section is having higher flexural capacity either when textile layers are farther from the neutral axis (2B > 2M) or tensile textile area is higher (2B > 1T1B). Moreover, the analytical values being lesser than the experimental values are preferable as it provides a more conservative estimate and is safe and adaptable for design. Having confirmed the analytical method with the help of experimental results, this now enables us to utilize the above set of formulae to calculate the flexural capacity of similar TRC cross-sections.

A crucial difference perceived between the $SP_{15}$ and $SP_{18}$ in the experimental behaviour is the difference of flexural capacity of 2M and 1T1B specimens from 2B specimens, as illustrated in Fig. 7. The difference is rather uniform for $SP_{15}$ and $SP_{18}$ analytically whereas the experimental values do not exhibit the same. The experimental flexural strength of 1T1B specimen varies more than 50% from 2B specimen, i.e., the flexural capacity is reduced more than half for 18 mm specimen whereas for 15 mm specimen the difference is only 25% between 2B and 1T1B. The difference of flexural strength between 2M and 2B specimens is almost similar for both $SP_{15}$ and $SP_{18}$ (19% and 12.6%). This can also be inferred with respect to volume fraction. For lesser volume fraction, the experimental difference in capacity of 1T1B configuration coincides with that of analytical calculations. This is further addressed in Fig. 8.

**Influence of Volume fraction**

From Fig. 6 (a & b), it is evident that the analytical method adopted provides reliable and similar results

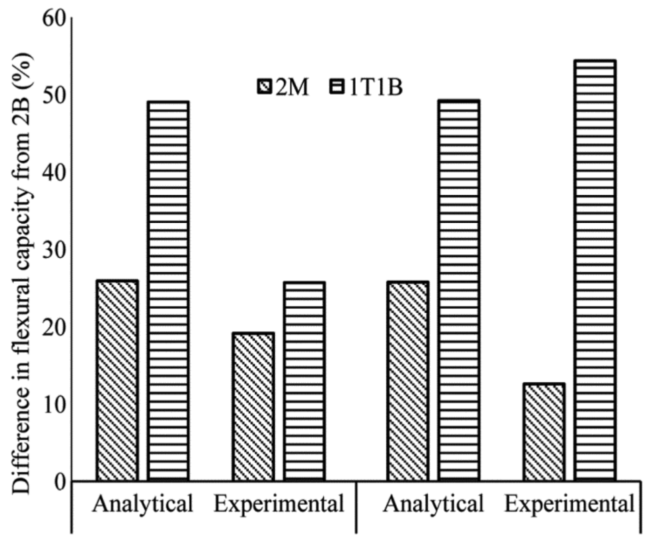


Fig.7 — Difference in flexural capacity from 2B

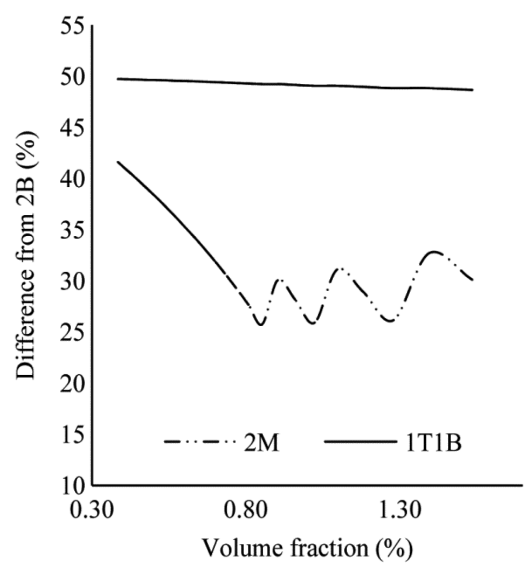


Fig. 8 — Difference in flexural capacity from 2B

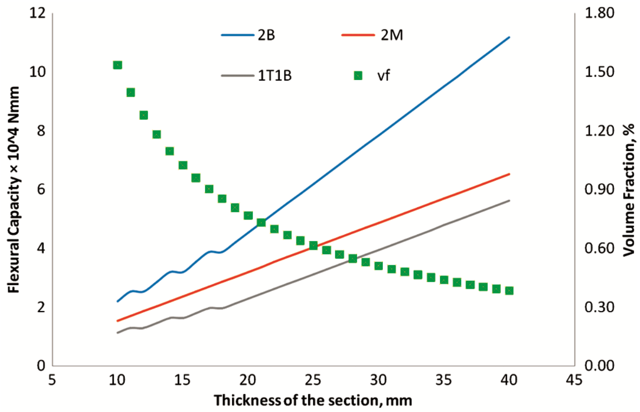


Fig. 9 — Flexural capacity of sections with various $v_f$ and layer positions

to that from experiments. Having established a relationship between analytical and experimental results, the investigation is carried out on the influence of volume fraction ($v_f$) of textile in matrix and textile position in flexural capacity. Employing the above-established relationship in Eq. (4), the flexural capacity of sections of different thicknesses, and for different $v_f$, for all the three positions of textile, is calculated as shown in Fig. 9. The variation of $v_f$ in various thicknesses and the corresponding flexural capacity of the section is plotted in Fig. 9, validating the benefit of placing the textile layers near the bottom, in the tension zone, over the other two textile placements for all $v_f$. This emphasizes that, although the material, its volume, and grade are identical, the difference in the capacity achieved from two different specimens which differ only by configuration is sizeable. Not taking such an advantage out of the structure would ultimately result in an uneconomical section. The immense difference in flexural capacity for lesser volume fraction is due to the increase in lever arm of rotation as the section depth increases. The $v_f$ decreases as the thickness of the section increases because the number of textile layers are maintained constant throughout various thicknesses. Since the increase in lever arm is maximum for 2B type, the capacity increases exceptionally for it. Although the increase in lever arm for 1T1B is equivalent in order of 2B, the textile area is lesser at tension zone, and hence increase in capacity is comparatively lesser. 2M, having a tensile textile area similar to 2B, has a lesser lever arm and thus lesser capacity than 2B. It can be inferred from the capacity of 2M and 1T1B of the same $v_f$, that, although lever arm could be manipulated to our advantage, a major contribution for flexural capacity is still from tensile textile area.

To understand the difference better, Fig. 8 illustrates this difference in the flexural capacity of 2M and 1T1B type from type 2B placement understandably. The difference is almost the same for the 1T1B type, around 50%, for all the thicknesses considered. This is as expected as it is merely similar to providing half the reinforcement in the tension zone as compared to 2B. Although the difference is fluctuating for smaller depths in the 2M type, the difference rises to be substantially large as the depth increases. The pattern of difference in flexural capacity for 2M type is distinctive as for higher $v_f$, i.e., depth till 18mm, the difference is around 30% and the difference continuously increases upon a further decrease in $v_f$. Both the results substantiate the earlier statement contemplating the influence of the textile area and lever arm. Although the lever arm for 1T1B is higher than 2M, the capacity is still higher for 2M. The slope of increase in the difference in flexural capacity for 2M continuously decreases and is not linear for both cases. We can effectively recognize that not only layer positioning, but also the volume fraction influences the flexural capacity of the section to a considerable extent.

The design implications primarily involve maximizing the capacity of the cross-section and achieving the most cost-effective design. When TRC is utilized in flexural applications, either as a flexural member or to strengthen existing members, manipulating the placement of the textile layer can provide significant advantages. In large-scale applications, maintaining the proper positioning of the textile layer can ensure the quality and consistency of the TRC product.

Another decisive benefit is the ability to cater to specific flexural demands by designing the most efficient section, which can greatly reduce the overall production expenditure. In large-scale manufacturing, employing such an efficient cross-section can result in substantial cost reduction by optimizing the materials involved.

## Conclusions

The study's goal was to determine the most advantageous layer position for a given volume fraction and examine the changes reflected in the flexural strength of TRC by varying the volume fraction for each of the layer positions considered. The experimental results established that providing textile layers near the bottom, at the tension zone is advantageous for flexural strength than providing them at the centre or equally distributed near both the ends. But providing a textile layer in the compression zone prevented the sharp fall in the strength of the section after reaching the ultimate load. After establishing analytical expressions agreeing with the experimental results, further analysis of the analytical values also corroborated the same. Without altering the actual composition or grade, significant additional flexural strength could be achieved purely by altering the layer position only. Although the advantage is about 20% for thinner sections, it is substantially high as higher depths are adopted. It is also recognized that the difference in flexural capacity from 2B is almost constant for 1T1B type for all volume fractions whereas, for 2M type, the difference is around 30% up-to volume fraction of 0.85% after which the difference consistently increases. It can also be realized that, although the tensile textile area predominantly participates in determining the flexural capacity of the section, the influence of the lever arm is substantial. As expected, the flexural capacity increases with an increase in lever arm as in the case of 2B but is also limited to the tensile textile area available as observed from 1T1B and 2M cases. The above study is limited to the flexural behaviour of the TRC members and future scope is extending the investigation applications involving tensile stress and TRC under the combined action of tension and flexure.

## References


1 Scheerer S, Chudoba R, Garibaldi M P & Curbach M, Shells made of textile reinforced concrete – applications, *J Int Assoc Shell Spat Struct*, **58** (2007) 79–93, https://doi.org/10.20898/j.iass.2017.191.846.

2 Quadflieg T, Goldfeld Y, Dittel G & Gries T, New age advanced smart water pipe systems using textile reinforced concrete, *Procedia Manuf*, **21** (2018) 376–383, https://doi.org/10.1016/j.promfg.2018.02.134.

3 Hegger J, Horstmann M & Zell M, Textile reinforced concrete – Realization in applications, *Proc Int FIB Symp*, (Amsterdam) 2008, 357–362.

4 Kulas C & Solidian, Actual applications and potential of textile-reinforced concrete, (2016) [https://www.semanticscholar.org/paper/Actual-applications-and-potential-of-concrete-Kulas-Solidian/0cafa4b696994d68afdc17604f69f236a8cb4137 (22 June 2021)]

5 Mendis P, Nguyen K T Q, Baduge S K & Chandrathilaka K, Textile reinforced concrete composite for advanced construction applications, *In Proceedings of the international conference on composites materials* (ICCM22), (Melbourne, Australia) 2019, 11–16.

6 Tsesarsky M, Katz A, Peled A & Sadot O, Textile reinforced concrete (TRC) shells for strengthening and retrofitting of concrete elements: Influence of admixtures, *Mater Struct*, **48** (2015) 471–484, https://doi.org/10.1617/s11527-013-0197-z.

7 Contamine R & Larbi A S, Development of a textile reinforced concrete (TRC) to retrofit reinforced concrete structures, *Eur J Environ Civ Eng*, **20(6)** (2015) 1–17. https://doi.org/10.1080/19648189.2015.1030089.

8 Bui T L, Nguyen X H & Si Larbi, A, In-Plane behavior of seismically damaged clay masonry walls repaired with external TRC, *Proc 4th Congrès Int de Géotechnique - Ouvrages –Structures*, (2018) 925–934, https://doi.org/10.1007/978-981-10-6713-6_92.

9 Akhoundi F, Vasconcelos G, Lourenço P, Silva LM, Cunha F & Fangueiro R, In-Plane Behavior of cavity masonry in fills and strengthening with textile reinforced mortar, *Eng Struct*, **156** (2018) 145–160, https://doi.org/10.1016/j.engstruct.2017.11.002.

10 Shams A, Hegger J & Horstmann M, An analytical model for sandwich panels made of textile-reinforced concrete, *Constr Build Mater*, **64** (2014) 451–459, https://doi.org/10.1016/j.conbuildmat.2014.04.025.

11 Shams A, Horstmann M & Hegger J, Experimental investigations on Textile-Reinforced Concrete (TRC) sandwich sections, *Compos Struct*, **118** (2014) 643–653, https://doi.org/10.1016/j.compstruct.2014.07.056.

12 Alrshoudi F A S, *Textile Reinforced Concrete: Design Methodology and Novel Reinforcement*, Ph D Thesis, The University of Leeds, Leeds, United Kingdom, 2015.

13 Gopinath S, Prakash A & Ahmed A K F, Flexural impact response and energy absorption characteristics of textile reinforced mortar, *Constr Build Mater*, **262** (2020) 120630, https://doi.org/10.1016/j.conbuildmat.2020.120630.